Unveiling genome plasticity and a novel phage in *Mycoplasma felis*: Genomic investigations of four feline isolates

Sara M. Klose[1,2*], Alistair R. Legione[1*], Rhys N. Bushell[3], Glenn F. Browning[1] and Paola K. Vaz[1]

*S.M.K. and A.R.L. have contributed equally to this work.

Affiliation:

1. Asia-Pacific Centre for Animal Health, Melbourne Veterinary School, Faculty of Science, The University of Melbourne, VIC, Australia

2. Institute of Molecular Medicine and Experimental Immunology, Faculty of Medicine, University of Bonn, NRW, Germany

3. Department of Veterinary Clinical Sciences, Melbourne Veterinary School, Faculty of Science, The University of Melbourne, VIC, Australia

Corresponding Author: Alistair Legione, legionea@unimelb.edu.au

Keywords: mycoplasma felis, whole genome sequencing, genome plasticity, evolution, phage

Repositories: All sequence data and assemblies for data associated with this project can be found under the GenBank Bioproject: PRJNA906261

Abstract:

We present the complete genomes of four clinical isolates of *Mycoplasma felis* from three domestic cats, assembled with the aid of short and long read sequencing methods. The completed genomes encode a median of 759 open reading frames (min, 743, max 777) and a median 98.2% average nucleotide identity to that of the available equid origin reference strain. Comparative genomic analysis revealed the occurrence of multiple horizontal gene transfer (HGT) events and genome reassortment. This resulted in the acquisition or loss of numerous genes within the Australian felid genomes, encoding putative proteins involved in DNA transfer, metabolism, DNA replication, host cell interaction, and restriction modification systems. Additionally, a novel mycoplasma phage was detected in one Australian felid *M. felis* isolate via genomic analysis and visualised via cryo transmission electron microscopy. This research identifies complex genomic dynamics and evolutionary adaptation of mycoplasmas to different host environments. Furthermore, the sequences obtained in this work are important for the development of new diagnostic tools, and identification of future infection control and treatment options for respiratory disease complex in cats.

Data summary:

All genome data for this study have been deposited in GenBank under BioProject PRJNA906261. Genome assemblies, as well as Illumina and Oxford Nanopore sequence reads for each isolate can be found under their respective BioSamples: SAMN32182834 (isolate 047), SAMN32182835 (isolate 219), SAMN32182836 (isolate 329), and SAMN32182837 (isolate 632). The authors confirm all supporting data and protocols have been provided within the article.

Impact statement:

Mycoplasma felis is commonly associated with clinical cases of conjunctivitis and feline respiratory disease complex in cats, the leading cause of euthanasia in shelters. In the absence of vaccines, infection control is currently limited to the prolonged use of antimicrobials. Prior to this study there was only one complete genome assembly of *M. felis*, which was isolated from a horse. The outcomes from this study marks the first high quality hybrid assembled genomes assembled from cats. This work adds four new genomes from clinical cases, as well as the identification and validation of the presence of a novel phage that utilises the mycoplasma translation table. The

52 genome data presented here can assist future projects investigating improved diagnostics and
53 development of new treatment options.
54

Introduction:

Mycoplasmas are the smallest free-living bacteria with the smallest bacterial genomes identified to date (0.58 – 1.38 Mb). Mycoplasmas are thought to approach the minimal gene sets essential for independent life, making them ideal model organisms for studies on the fundamental requirements of a living cell [1]. Mycoplasmas evolved from Gram positive bacterial ancestors 600 million years ago [2], and have undergone rapid genome reduction during evolution [3, 4]. They are cell wall-less, Gram negative pleomorphic bacteria and can be found to infect and cause both acute and chronic disease in a diverse array of animal and plant species [5].

Mycoplasmas are known for their rapid evolution and genetic plasticity, mainly driven by intra-species spontaneous mutation or horizontal gene transfer (HGT) between and within species, facilitating swift adaptation to environmental changes and enhancing survival and/or virulence [6-9]. Studies examining the genomic stability of *Mycoplasma synoviae* revealed that it not only undergoes frequent mutations in birds [10], but also manifests rapid thermoadaptive evolution *in vitro* and *in vivo* [11], presumably to regain fitness and pathogenicity [12, 13]. HGT is observed to occur more frequently between species that share an ecological niche irrespective of their phylogenetic divergence, such as transfer of surface VlhA lipoprotein involved in phase variation from *Mycoplasma gallisepticum* to *M. synoviae* infecting poultry [14], and transfer of several surface lipoproteins involved in host colonisation from *Mycoplasma capricolum* subsp. *capricolum* and *Mycoplasma mycoides* subsp. *mycoides* to *Mycoplasma agalactiae*, infecting ruminants [15].

There have been at least four species of mycoplasmas isolated from cats (*Mycoplasma felis*, *Mycoplasma gatae*, *Mycoplasma arginini*, and *Mycoplasma feliminutum*), in most cases as common commensal microflora, but they have been associated with conjunctivitis and, increasingly, feline respiratory disease [16-19]. Feline respiratory disease complex (FRDC) in cats is the leading cause of euthanasia in animal shelters [20] and is commonly associated with several viral (feline herpesvirus 1 and feline calicivirus) and bacterial pathogens, including *M. felis* [21, 22]. *M. felis* infections are common in most cat populations and their ability to establish chronic persistence in an animal enhances opportunities for recurring opportunistic infections. Vaccines against *M. felis* are not currently available and treatment is limited to the prolonged use of antimicrobials in the tetracycline and fluoroquinolone classes [23, 24]. Currently there are three isolates with full

genomes published for this species: strain Myco-2 (GenBank accession number: AP022325.1), an isolate from a case of respiratory disease in a horse in Japan [25] which has been completely assembled, and multiple assemblies of isolates 16-040612-4 (CP104192, CP104193, CP104194, CP11027) and 16-057065-4 (CP103988, CP103993, CP110269), which were each isolated from feline bronchoalveolar lavage in Canada [26]. Additionally, there is an incomplete ATCC strain (ATCC 23391) assembled into scaffolds (GenBank Biosample: SAMN02841218).

This report describes four high quality, complete, *M. felis* genomes, the first that have been generated using hybrid assembly methods. These genomes also represent the first complete assembly of feline isolates of this species. Additionally, we have identified and visualised a novel mycoplasma phage, which utilises mycoplasma codons. This report represents a significant expansion on our limited understanding of the genomic structure and plasticity of *M. felis*. Such work may lead to enhanced development of diagnostic tests and vaccines, as has been seen in other mycoplasma species.

Methods:

Microbial isolation

Swabs were taken for bacteriological culturing from clinical cases of respiratory disease (3 cases) and an unresolved post-surgical infection (1 case) (Table 1). Swabs were spread onto aerobic Sheep Blood Agar (SBA) plates and incubated at 37°C. Following observation and presumptive identification of small mycoplasma-like colonies, single colonies were transferred to Mycoplasma Broth (MB) containing 10% swine serum (Sigma-Australia) and 0.01% nicotinamide adenine dinucleotide (NAD) (Sigma-Australia) based on a formulation of Frey's medium with minor modification [27, 28]. Acidification of MB media was used to confirm the growth of *Mycoplasma* spp. and the cultures were stored at -80°C for future investigations.

DNA extraction, sequencing, and genome assembly

Bacterial isolates were cultured axenically in MB for 18 hours at 37°C prior to DNA extraction. Bacteria were pelleted and media removed, followed by resuspension in extraction kit specific lysis buffers. The DNA for short read sequencing was extracted using the DNeasy Blood and tissue kit (QIAGEN) following the manufacturer's protocol. Following this, 100 ng of extracted DNA was used

117 to prepare sequencing libraries using Illumina's Nextera Flex DNA library prep kit. Sequencing was
118 performed on the NovaSeq platform at Charles River Laboratories, Victoria, Australia, to generate
119 150 bp paired end reads. Two batches of Oxford Nanopore Technologies (ONT) long read
120 sequencing were performed. The DNA was extracted using the Promega Wizard® DNA Purification
121 Kit (Batch 1) or the Promega Wizard High Molecular Weight DNA Purification Kit (Batch 2). In both
122 instances DNA libraries were generated using the ONT Rapid Barcoding (SQK-RBK004) kit.
123 Sequencing was performed on a MinION Mk1b device fitted with a FLO-MIN106D flow cell (R9.4.1
124 chemistry). Base calling, demultiplexing, and adapter removal utilised Guppy (version
125 6.2.1+6588110a6) high accuracy base caller and a minimum quality score of 9 (default settings).
126
127 The Illumina reads were trimmed and adaptors removed using fastp v0.20.1 [29] using default
128 settings. The ONT reads from the two batches were merged per isolate and processed through
129 Filtlong v0.2.0 [30] to remove all reads shorter than 1000 bp and retain 90% of input data
130 (removing short and low quality reads). Subsequently, the processed short and long reads were
131 used as input into Unicycler v0.5.0 [31] in 'normal' mode, with a modified start gene database to
132 include *M. felis*. The assemblies where then polished using Polypolish v0.5.0 [32], incorporating
133 BWA-MEM v0.7.17-r1188 [33]. Full genome alignments were generated using the progressive
134 MAUVE algorithm [34] to identify regions of reassortment and gene loss or gain.
135
136 *Genome annotation and sequencing analysis*
137 Genomes were annotated using the Prokaryotic Genome Annotation Pipeline v2022-12-
138 13.build6494 [35] for primary analysis. A Tenericutes specific protein database was downloaded
139 from UniProt containing both Swiss-Prot (4464 sequences) and TrEMBL (343,598 sequences)
140 annotations and converted to a diamond format protein database [36]. This database was used as
141 input to Pydeel (https://github.com/alegione/pydeel) to determine the coding ratio of our
142 annotated genomes compared to *M. felis* genomes on GenBank. This tool identifies the coding ratio
143 of annotated genes compared to their best hit within the provided database to identify the
144 proportion of annotated genes that may have erroneous insertions or deletions as a by-product of
145 the use of long read sequencing. From here, annotated genomes were processed through Panaroo
146 v1.3.0 [37] along with previously sequenced *M. felis* genomes (Myco-2 and ATCC23391) to identify
147 the core genome. The core genome results were visualised using Pagoo [38]. The annotated
148 genomes from this study were investigated for pathogenicity islands, and integrative conjugative

149 elements using Island Viewer 4 [39], and ICE finder [40], respectively. Antimicrobial resistance
150 genes and virulence factors were analysed by generating a Diamond database of the CARD [41] and
151 full virulence factor databases [42], and using Diamond BLASTp to identify best hits with a cut off
152 bit score of 50. The UniProt webserver was used to identify homologs of specific open reading
153 frames (ORFs) in other genomes (https://www.uniprot.org).
154
155 *Phage isolation and visualisation*
156 A phage-like contig was identified in the annotation results of one of the assemblies (MF329). In
157 order to confirm if the detection of bacteriophage genomic sequence corresponds to integrated
158 prophage or to replicative virions, bioinformatic methods were first utilised. The probable terminal
159 ends were investigated through short and long read mapping to the contig using BWA-MEM and
160 minimap2 v2.26-r1175 [43], respectively, and the contig's starting point adjusted based on the
161 depth of coverage. The tool PhageTerm [44] was also utilised to investigate the potential phage
162 start/end point. To investigate whether this contig was a prophage the long reads were mapped,
163 using minimap2, to the updated phage contig. Any reads that had overhangs at the 5' and 3' end of
164 the contig were extracted and subsequently mapped to the MF329 assembled genome to
165 determine if there was a common point of overlap.
166 To determine the presence of productive bacteriophage virions, transmission electron microscopy
167 was performed on cultured MF329. Isolate MF329 was cultured in 50 mL of axenic mycoplasma
168 media as described above for 20 hours. The bacterial culture was centrifuged for 15 mins at 10,000
169 x g at 4°C and the media fraction separated from the bacterial cell pellet. The bacterial cells were
170 gently lysed by resuspension in 150 uL of sterile water, followed by centrifugation at 10,000 x g at
171 4°C for 5 mins to remove cellular debris. This was repeated twice, with supernatant fraction
172 captured each time for ultracentrifugation. The culture media and the cell lysate supernatant
173 fractions were separately ultra-centrifugated at 100,000 x g for 90 mins at 4°C, and pellets
174 resuspended in 0.2 M HEPES buffer, pH 7.7. Samples were inspected and visualised by negative
175 staining at the Ian Holmes Imaging Center (Melbourne, Australia) using a FEI Talos L120C cryoTEM
176 (Talos L120C) microscope.
177
178
179 **Results:**

180 *Genome characterisation and comparisons*

181 All four isolates were successfully assembled into circularised, complete genomes. In addition to
182 these four genomes, a novel phage genome of *M. felis*, was identified that utilised the Mycoplasma
183 translation table. Metrics for long and short read sequencing output are available in Table 2. The
184 assembly statistics for the four isolates are available in Table 3. Briefly, the circularised isolates
185 were sufficiently larger than the reference genome (Myco-2; 841,695 bp), with a median length of
186 940,935 bp (range: 905,741 – 948,716) and a median of 759 coding domain sequences (CDS)
187 (range: 743 – 777) compared to the reference genome which has 740. The NCBI Prokaryotic
188 Genome Annotation Pipeline incorporates a CheckM [45] completeness analysis and an average
189 nucleotide identity taxonomic classification step to identify any potential issues with an assembled
190 genome. For all four cases CheckM completeness mirrored the reference genome Myco-2 (99.21%
191 completeness), and all assemblies were classified as *Mycoplasma felis* with high confidence (Table
192 3). The coding ratio of annotated assemblies were investigated to identify the frequency of
193 potential indel errors. Two published *M. felis* genomes (Myco-2 and ATCC23391) had a mean
194 coding ratio of 1.0 (Standard deviation ±0.02) and 0.96 (±0.32), respectively. Our completed
195 genomes, MF47, MF219, MF329, and MF632 had mean coding ratios of 1.0 (±0.28), 0.99 (±0.30),
196 1.0 (±0.27), and 1.0 (±0.26), respectively. Seven recently sequenced *M. felis* isolates that utilised
197 only Oxford Nanopore sequencing had a substantial number of indel errors in their annotations
198 based on coding ratio analysis (mean coding ratio between 0.44 and 0.47) and were not used in
199 further comparisons for this reason (Figure 1).

200

201 Two isolates, MF047 and MF632 had an additional tRNA compared to the remaining isolates, for
202 tRNA-Trp and an unknown tRNA respectively. The newly sequenced isolates had 1-3 secretory
203 systems (in all cases these were annotated as Type IV secretory systems), whilst Myco-2 has no
204 annotated secretory systems. The newly annotated sequences also and an increased number of
205 transposases, typically annotated as IS1634 or IS256, and IS3 in a few cases. By comparison Myco-2
206 only had IS3 and IS1634 family transposase annotations.

207

208 A progressive MAUVE alignment of the four assemblies in comparison to Myco-2 (Figure 2)
209 identified two significant genome inversions in the reference sequence compared to the isolates
210 assembled here, as well as more localised inversions between each of the isolates. These
211 inversions, along with genomic regions present in individual isolates, were typically flanked by

212 transposases. Comparison of ANIs between the four new assemblies, and previously published *M.*
213 *felis* genomes (Table 4) found that all four Australian isolates' best match was to another isolate
214 from this study besides MF329 (MF047 and MF219, 99.8%; MF632 and MF329, 98.3%, MF329 and
215 ATCC23391 98.4%), noting that MF047 and MF219 originated from the same animal two months
216 apart.
217
218 The core genome of *M. felis* as determined by Panaroo (genes present in >99% of genomes)
219 contained 595 genes, with 301 shell genes (genes present in 15% - 95% of genomes). Collapsing
220 paralogues increased the core genes by one and reduced the shell genes to 219. Principal
221 component analysis (PCA) highlighted clustering of the two published genomes, as well as
222 clustering of isolates that were taken from the same individual (Figure 3). All genes, besides those
223 annotated as hypothetical proteins, identified in newly sequenced isolates but not present in the
224 reference sequence are present in Table 5, including the homologs found in other genomes. The
225 variations between the genomes were mostly observed in sequences encoding putative proteins
226 involved in DNA transfer, metabolism, DNA replication, mycoplasma-host cell interaction, and
227 restriction modification systems (Figure 4).
228
229 *Genomic islands, virulence genes, antibiotic resistance genes*
230 Genomic islands were detected in three out of the four sequenced genomes (Table 7). The average
231 length of these islands was 22,145 bp (±5818 bp) and each contained an average of 16 (±5)
232 annotated genes. In comparison, the Myco-2 strain of *M. felis* had two predicted genomic islands of
233 3052 bp and 10,027 bp length. Further inspection of these predicted genomic islands identified
234 matching regions present in isolates in alternative locations. For example, MF329 had a 24 kb
235 (311,409 – 335,810 nucleotide position [nt]) predicted genomic island containing 19 genes
236 including a type IV secretion system and an insertion sequence (IS1634) at its midpoint. Extraction
237 and remapping of this genomic island found that it was repeated three times within a wider 122 kb
238 region (213,995 – 335,810 nt) of the MF329 genome. Of these repeated regions, only the predicted
239 genomic island repeat contained the IS element. This same region occurred without the IS element
240 present in MF047 (twice), MF219 (once), and MF632 (once). In the case of MF632, the region was
241 also a predicted as a genomic island, but in this instance was flanked with restriction endonucleases
242 and either predicted transposases (3') or an IS256 element (5').

243 Diamond BLAST searches for antibiotic resistance genes and virulence genes resulted in
244 identification of few high identity hits (Table 6 and Supplementary Tables 2 and 3). Only one hit to
245 the virulence factor database had an amino acid identity greater than 90%, predicted to encode for
246 the adherence virulence gene elongation factor Tu in *Mycoplasma synovia* (90.1% average identity)
247 and was present in all genomes. Below that, the only five genes had hits with >50% amino acid
248 identity. The closest hits to these genes were oppF (59.9% identity; *Mycoplasma mycoides* subsp.
249 *Mycoides*; Immune modulation), eno (58.9%; *Streptococcus pneumoniae*; Exoenzyme), gap (57.9%;
250 *Mycoplasma genitalium*; Adherence), dnaK (53.9%; *Chlamydia trachomatis*; Adherence), and sugC
251 (50.4%; *Mycobacterium marinum*; Nutritional/Metabolic factor). No genes had hits with >50%
252 amino acid identity with antibiotic resistance genes in the CARD database.
253
254 *Phage/Prophage detection and identification*
255 A 33.6 kb contig (vB Mfe PM329; *Mycoplasma felis* strain PM329) was assembled and identified as
256 a likely phage or prophage within the sequenced *M. felis* MF329 isolate. It had an average depth of
257 coverage of 40,847.7 reads, with 82.6% of Illumina MF329 reads mapping to phage genome.
258 Interrogation of the nanopore read dataset to determine genome integration status detected only
259 63/18134 (0.35%) reads mapping to both phage and bacterial genome. Of these, most were found
260 to map across the bacterial genome at mostly single-read depth, with the exception of five reads
261 which clustered mid-genome in the region of 456,500 nt. If this were to be indicative of a true
262 insertion site it would likely disrupt ORF MF329_000403, encoding a putative 16S rRNA
263 pseudouridine synthase gene. The phage genome has a 27.1% G+C content and encodes 36
264 predicted ORFs using the mycoplasma translation table. It shared 94.8% nt global pairwise identity
265 with that of two nanopore contigs in the publicly available unassembled *M. felis* contig dataset
266 (NCBI Biosample: SAMN30346842), and 96.8% and 97.4% aa pairwise identity between their
267 encoded putative recombinase and portal proteins, respectively. Interrogation of the read datasets
268 of the other three isolates sequenced in this study identified only 4/9515 (0.04%; MF047),
269 19/19128 (0.1%; MF632) and 22/65383 (0.03%; MF219) mapped nanopore reads, within the range
270 of barcode error, and no Illumina reads mapped to the phage genome, indicating those isolates
271 were not carrying the phage. Phylogenetic analyses via VipTree [46] and vContact2 [47] was not
272 able to assign vB Mfe PM329 to any known phage genus or family, however gene arrangement was
273 found to be similar to those of the MAgV1 from *M. agalactiae* and MAgV1-like prophage sequences
274 described in mycoplasma species of the Hominis phylogenetic host group. In particular, both

275 protein and gene arrangement similarity were greatest to those in prophage encoded within *M.*
276 *mustelae* and *M. molare*, including a central position of the recombinase gene. BLASTX analysis of
277 predicted ORFs detected protein pairwise identities of 48% to 69% between core conserved ORFs
278 encoded within the *M. mustelae* and *M. molare* prophage sequences [48] (**Error! Reference source**
279 **not found.**).
280
281 Confirmation of productive virus formation was performed by cryoTEM on media and cell lysate
282 supernatant fractions, revealing the presence of non-enveloped contractile-tailed polyhedral viral
283 particles of approximately 100 nm in length, with a 50 nm diameter head and tails of varying
284 lengths observed. Higher numbers of virions were observed within the cellular lysate supernatant
285 fraction than in the culture media fraction, with clusters of virions seemingly embedded within
286 bacterial membrane debris observed (Figure 5). These long tailed polyhedral viral structures are
287 consistent with those possessed by siphoviruses and myoviruses found within the recently ratified
288 *Caudoviricetes* class of bacteriophage. The contractile tail and polyhedral head structure is
289 consistent across all visually elucidated mycoplasma phages, with the main differences
290 corresponding with head and tail lengths. *M. pulmonis* Phage P1 has a 28 nm isometric head and
291 short tail, Br1 has 77 nm head diameter and a 104 nm long tail [49], and *M. hyorhinis* Hr1 phage, is
292 a short-tailed (14nM) phage with a 34 nm head [50].
293

294 ## Discussion

295 In this study, genomic characterisation of four new *M. felis* isolates was performed; three derived
296 from clinical cases of respiratory disease and the remaining from an unresolved post-surgical
297 infection. Comparisons that included several published datasets detected genomic variations and
298 inversions between the Australian felid isolates and the only assembled *M. felis* reference equid
299 isolate, prominently flanked by transposases which is indicative of HGT and genome reassortment.
300 This includes differences detected in the number of copies of several encoded putative transposase
301 families, such as IS1634, IS256 and IS3 family transposases (Figure 4). Insertion sequences (ISs) are
302 transposable elements often present in multiple copies in a genome and involved in chromosomal
303 rearrangements by deletion, insertion, or inversion. The substantial similarity between various
304 isoforms of ISs enables them to facilitate DNA homologous recombination [51]. IS families encoded
305 in mycoplasma genomes play an important role in genome plasticity with several reported

306 instances of IS exchange between strains or species [15, 52-55]. This is in contrast to early research
307 that suggested some ISs, such as IS1634 which was in abundance in our sequenced genomes, were
308 unique to specific mycoplasma species [56]. The dissimilarity of the Australian felid genomes
309 obtained from three different cats, based on gene presence/absence and the number of coding
310 sequences, underscores the genetic diversity present amongst sequenced felid isolates (Figure 3) as
311 a result of the acquisition or loss of numerous genes within their genomes. Multiple gene
312 insertions, relative to the equid reference genome, were identified within the cluster of Australian
313 field isolates (Table 5). This includes genes involved in DNA transfer, replication, metabolism,
314 restriction modification (RM) systems, as well as various proteins of unknown function (Figure 4).
315
316 *Gene gains compared to the equid reference strain*
317 Of particular interest are those gene acquisitions involved in DNA transfer, such as the detection of
318 several copies encoding the putative type IV secretory system (T4SS) conjugative DNA transfer
319 family protein within the Australian felid genomes, with none detected in the publicly available
320 equid and felid genomes. T4SS conjugation systems translocate DNA through a process dependent
321 on cell to cell contact and have been identified as one of the core genes within Integrative and
322 Conjugative Elements (ICEs) in mycoplasmas, which play a significant role in genome plasticity of
323 these bacteria [57, 58]. ICEs have been shown to be self-transmissible in *M. agalactiae* providing
324 conjugative properties from ICE-positive cells to ICE-negative cells, while chromosomal transfers
325 (CTs) occur in the opposite direction at the same time [59]. Protein sequence analysis of the
326 putative T4SS identified in the Australian feline isolates showed 43.2% identity to the ORF5 of ICE in
327 *Mycoplasma cynos*. Whilst *M. cynos* predominantly infects the respiratory tract of dogs, it has also
328 been detected in cats in association with conjunctivitis and upper respiratory tract disease [60].
329 Taken together, it is plausible that a potential HGT event may have occurred to transfer the T4SS
330 conjugative element of ICE from an *M. cynos*-like species to *M. felis* in a shared feline host. This
331 T4SS was part of a defined region of genes that, along with 15 hypothetical proteins and a DUF87
332 domain-containing protein, was repeated three times in MF329. DUF87 domain-containing proteins
333 are associated with conjugative elements in other organisms such as TraJ in the virulence plasmid
334 of *Salmonella enterica* serovar Typhimurium [61], adding further weight to the likelihood of this
335 being an ICE, despite the bioinformatics tools utilised here not detecting it as one.
336

337 Several genes involved in metabolism were newly detected in felid isolates sequenced in this study.
338 A type 2 glycerol-3-phosphate oxidase (GlpO) was identified within the Australian genomes, while
339 in the equid isolate, only its FAD-dependent oxidoreductase domain was detected, accompanied by
340 two transposases located upstream. GlpO converts glycerol-3-phosphate to dihydroxyacetone
341 phosphate (DHAP) releasing hydrogen peroxide as a by-product which has been shown to play a
342 role in *in vitro* cytotoxicity of *M. gallisepticum* and *Mycoplasma pneumoniae* [62, 63], and virulence
343 of *M. mycoides* subsp. *mycoides* small colony and mosquito-associated *Spiroplasma* species [64,
344 65]. The significant reduction or complete loss of H_2O_2 production in highly passaged *M. bovis*, *M.*
345 *agalactiae*, *M. gallisepticum*, and attenuated vaccine strains of *M. gallisepticum* compared to wild
346 type strains suggests that glycerol metabolism capabilities can rapidly become redundant [62, 66,
347 67]. It is possible that the sequences coding for GlpO was lost in the equid *M. felis* isolate possibly
348 due to different levels of available glycerol as the nutrient source, or an altered pathogenicity in
349 horses compared to cats. Likewise, variations in the gene counts coding for nutrient transport
350 systems were observed, including ATP-binding cassette (ABC) transporters and the PEP-dependent
351 phosphotransferase transport system (PTS), as well as numerous other metabolic enzymes amongst
352 the Australian and equid isolates. A number of these nutrient transport systems, and many cell
353 surface enzymes are multifunctional in mycoplasmas playing critical roles in pathogenesis and
354 survival in the host [13, 68-73]. The differences observed in the PTS and ABC transporters of the
355 Australian felid isolates, in contrast to the equid isolate, may also be indicative of rapid metabolic
356 gene gains and losses occurring in response to the varying nutrient availabilities within their felid
357 and equid ecological niche.
358
359 In the Australian felid genomes, five new coding sequences related to replication were identified
360 which were absent in the equid origin genome, including genes responsible for putative anti-
361 termination protein NusB, Hsp70 family protein, C5 methylase, 16S rRNA methyltransferase RsmG,
362 and HNH endonuclease. The presence of these additional proteins suggests a potential difference in
363 bacterial growth within the feline host as compared to the equine host, potentially due to distinct
364 replication strategies. Future experiments comparing growth patterns of these isolates in felid or
365 equid derived cells are indicated. The potential origins of these additional sequences have
366 frequently been detected in mycoplasmas isolated from mink, swine, and dogs, which share a
367 common ecological environment with cats, or pigeons which are a common prey for cats. The HGT
368 events resulting in the acquisition of these genes by the Australian *M. felis* felid isolates may have

369 been facilitated by the close ecological proximity or may have occurred within the feline
370 gastrointestinal tract (GI) following the ingestion of the infected prey. HGT among diverse
371 microorganisms within the mammalian GI tract is frequently observed, possibly due to the physical
372 proximity it provides, thereby facilitating genetic exchange [74]. Furthermore, the conjugation
373 mechanism favoured for HGT within the GI tract protects DNA from nucleases and heavy metals,
374 and thus results in a successful genetic exchange [75].
375
376 Two additional restriction endonucleases (Eco47II and Sau3AI) were detected in the Australian felid
377 genomes, and the loss of a DpnII family type II restriction endonuclease. Restriction modification
378 (RM) systems play a pivotal role in regulating the bacterial HGT by protecting the genome against
379 incoming mobile genetic elements, or by facilitating recombination of the invading DNA [76]. A
380 strong correlation has been reported between the presence of active Type II RM systems and the
381 presence of mobile genetic elements and ICEs within *M. agalactiae* genomes, indicating the
382 facilitative role of Type II RM systems in HGT in mycoplasmas [77]. Furthermore, the diversification
383 of RM target recognition sites can regulate HGT by promoting gene exchanges among those with
384 RM systems that recognise the same target motifs, and by reducing gene transfer between lineages
385 that possess distinct RM systems [78]. Taken together, it is plausible that following a host switch
386 into horses, *M. felis* may have diversified their RM systems to enhance the level of genetic
387 exchange from phylogenetically distant bacteria, especially in cases where genetic exchanges were
388 previously restricted.
389
390 *Gene losses compared to the equid reference strain*
391 A sequence encoding a putative ComEC/Rec2 family competence protein has been observed to be
392 absent in the Australian felid isolates. This protein is one of the components of DNA translocation
393 via transformation enabling DNA transport by forming a channel across the cytoplasmic membrane
394 [79]. While ComEC component has been reported essential for DNA transport in Gram positive
395 bacteria, deletion of homologous genes did not affect DNA uptake in cell wall-deficient bacteria
396 [80]. Furthermore, the competence domain seems to be missing in many mycoplasmas possibly
397 due to the reductive evolution of these bacteria [81]. Characterisation of two mycoplasma genomes
398 recovered from gut microbiota of a deep-sea isopod detected *comEC* gene adjacent to genes
399 encoding enzymes producing dTMP from thymidine or dUMP, suggesting that the role of ComEC
400 protein might be importing extracellular DNA as a nutrient source [82]. The presence of ComEC in

401 the *M. felis* equid isolate, but its absence in the Australian felid isolates suggests that during the
402 evolutionary process the DNA translocation approach via a membrane channel might have been
403 made redundant and perhaps replaced with T4SS conjugation-mediated tactics as discussed above.
404
405 The Australian felid genomes exhibited a total absence of four coding sequences involved in host
406 cell interaction, namely those encoding putative variable surface lipoprotein, fibronectin type III
407 domain-containing protein, FIVAR domain-containing protein, and GA module-containing protein,
408 in contrast to the equid genome. The FIVAR (Found In Various Architectures Region) and GA
409 domains serve as essential constituents of the extracellular matrix-binding protein (Embp),
410 facilitating biofilm formation and attachment to fibronectin in some bacteria such as
411 *Staphylococcus epidermidis* and *S. aureus* [83, 84]. The presence of more than 30% similarity in
412 protein sequences between the FIVAR domain and GA protein in the equid *M. felis* reference Myco-
413 2 isolate, in comparison to the domains found in Embp of *S. aureus*, raises the possibility that the
414 equid isolate might have retained the potential for biofilm formation and/or fibronectin
415 attachment during the genome reductive evolutionary transition from Gram-positive bacteria.
416 Conversely, the absence of these proteins, in addition to the surface lipoprotein and fibronectin
417 type III domain-containing protein, suggests that these capacities may have become obsolete in the
418 Australian *M. felis* isolates infecting feline hosts, possibly indicating a different mode of host cell
419 interaction following the host switch.
420
421 *Rapid evolution within two months in one host:*
422 Two of the Australian *M. felis* isolates sequenced in this study, MF047 and MF219, were obtained
423 from separate bronchoalveolar lavages (BAL) of a feline patient presenting clinical signs consistent
424 with pneumonia. MF047 was isolated from the BAL taken at initial consultation, whereafter
425 treatment with 25 mg of doxycycline was administered twice a day orally for approximately two
426 months. Due to an unsatisfactory response to treatment, a second BAL was taken and MF219 was
427 isolated. While no genome reassortment was detected between the MF047 and MF219 genomes,
428 minor differences were observed in the counts of some genes encoding proteins involved in RM
429 systems, DNA transfer, and methylation (Figure 4). These variations may suggest a rapid host
430 adaptation of *M. felis* after only two months. The growing utilisation of whole genome sequencing
431 in mycoplasma diagnostics is revealing links between genetic mutations and antimicrobial
432 resistance. Genomic comparison of MF047 and MF219 revealed the presence of five single

433 nucleotide polymorphisms (SNPs) within the gene encoding ribosomal RNA small subunit
434 methyltransferase A (RsmA/KsgA), along with one SNP in the gene responsible for 16S rRNA and
435 another SNP in the gene responsible for 23S rRNA. In other studies, mutations within the 16S RNA
436 methyltransferase family have been reported to confer aminoglycoside resistance in *M. bovis* and
437 *M. gallisepticum* [85, 86], while mutations in the 16S rRNA or 23S rRNA genes have been shown to
438 be associated with resistance to tetracyclines in *M. pneumoniae*, *M. hominis*, *M. genitalium*, and *M.*
439 *bovis* [85, 87-89]. Both MF047 and MF219 contained five protein coding regions with low
440 confidence matches to tetracycline resistance genes, with the highest bit score of the five
441 associated with a predicted elongation factor G protein with an amino acid identity/similarity to
442 *tet*(T) from *Steptococcus pyogenes* of 25.8%/47.7%. It is important to emphasise that the
443 application of novel genome sequencing techniques for mycoplasma diagnostics, particularly in the
444 context of antimicrobial resistance, is still in its early stages, and the availability of data for
445 comprehensive analysis covering all mycoplasma species (particularly animal mycoplasmas) is
446 currently limited. Future research involving susceptibility testing of isolates MF047 and MF219 to
447 tetracyclines is necessary to determine whether there is a correlation with the observed genomic
448 variations and tetracycline resistance.
449
450 *Phage in mycoplasmas*
451 In other bacteria, phage have been demonstrated to provide critical virulence factors to their hosts,
452 required for the pathogenic activity of diverse bacteria (e.g. cholera, diptheriae, botulism, shiga
453 toxin-producing *E. coli*, etc). Approximately 20 mycoplasma-infecting phage/prophage have been
454 reported across diverse ruminant, avian, canine, swine, human and rodent mycoplasmas [48, 90].
455 Of these, most are unclassified, only three have had their virion structure visualised (P1, Hr1 and
456 Br1), and only one has been classified by the International Committee for the Taxonomy of Viruses
457 (ICTV). That is, the temperate *M. pulmonis* phage P1 (12 Kb genome), as the sole member of the
458 floating genus *Delislevirus* [91]. The well-described MAV1 temperate phage found in *M. arthritidis*
459 (16 Kb genome) has not yet (at time of publication) been classified within the new system. In other
460 mycoplasmas, phages have demonstrated dynamic mobility within the bacterial chromosome, loss
461 of integrated phage with clonal passage (MFV1 in *M. fermentans*), and variable expression of
462 unique phage-encoded membrane surface proteins (MFV1 and MAV1, in *M. fermentans* and *M.*
463 *arthritidis*, respectively) [92] with a potential role in bacterial adaptation and survival. Detection of
464 a similar contig within *M. felis* 16-057065-4 (NCBI Biosample: SAMN30346842) from Canada

465 indicates that this phage is likely carried by *M. felis* strains globally, although in that study it was not
466 identified as a phage/prophage but as *M. felis* bacterial genomic DNA. No known selective
467 advantage or disadvantage to the presence of this phage within *M. felis* was determined as part of
468 this study due to the low number of available *M. felis* genomes. Future epidemiological studies to
469 investigate the potential role of phage carriage in feline mycoplasma-associated disease cases is
470 indicated.
471
472 Conclusions
473 This study presents a comprehensive analysis of the first high-quality, complete *M. felis* genomes
474 isolated from cats, along with the characterisation of a novel mycoplasma phage. It provides
475 valuable insights into the intricate genomic dynamics of *M. felis*, showcasing a complex interplay of
476 gene gains, losses, horizontal gene transfer events, and adaptations to new host environments.
477 These findings suggest divergent evolutionary paths in different hosts and offer compelling avenues
478 for further research into the evolutionary mechanisms and ecological factors that influence the
479 genomic diversity of mycoplasmas.
480
481

482 Conflicts of interest:

483 The author(s) declare that there are no conflicts of interest.
484

485 Funding information:

486 This study was supported by the Feline Health Research Fund. P.K.V. was supported by a University
487 of Melbourne, Melbourne Postdoctoral Fellowship.

488

489 Author contributions:

490 R.N.B. performed the bacterial isolation and initial classification; A.R.L., S.M.K. and P.K.V. prepared
491 the DNA samples, performed the sequencing and analysis; P.K.V. isolated the phage for TEM; P.K.V.,
492 S.M.K., G.F.B. and A.R.L. conceptualised the study design; P.K.V., S.M.K. and A.R.L. acquired the
493 funding; S.M.K., A.R.L. and P.K.V. drafted the manuscript, and R.N.B. and G.F.B. revised the
494 manuscript.
495

Acknowledgments:

The authors would like to gratefully acknowledge the small animal medicine team of the U-Vet Werribee Animal Hospital at The University of Melbourne, for providing the samples taken from clinical cases, and Eric Hanssen at the Ian Holmes Imaging Centre for the cryoTEM imaging of vB Mfe PM329 phage.

503 **Table 1.** *Mycoplasma felis* isolates sequenced in this study.

Isolate	Month/Year	Animal ID	Clinical case	Isolation site	Other notes	Genbank #
047	3/2015	Cat A	Pneumonia	Respiratory, BAL	Heavy growth from BAL, treated with Doxycycline	CP114890
219	5/2015	Cat A	Pneumonia	Respiratory, BAL	Follow-up isolation from Cat A	CP114889
329	5/2014	Cat B	FRDC	Respiratory, BAL	Chronic bronchitis. PCR negative for herpesvirus, calicivirus and chlamydia	CP115656 OR753717 (phage)
632	12/2010	Cat C	Surgery	Fat tissue	Isolated from non-healing surgical wound	CP114888

504 BAL, Bronchioalveolar lavage; PCR, polymerase chain reaction; FRDC, feline respiratory disease complex

505

506 **Table 2.** DNA sequencing results summary after trimming and quality filtering

	MF047	MF219	MF329	MF632
Illumina reads				
Total paired reads	8,977,712	6,647,214	6,481,506	6,807,888
Median length	151	151	151	151
>Q20 (%)	96.93	95.7	96.83	96.99
>Q30 (%)	91.31	88.43	91.12	91.41
GC (%)	24.64	24.67	26.35	24.85
Nanopore reads[^]				
Total reads	65,383	9,515	103,977	19,128
Median length	7,049	6,563	3,717	5,058.5
N50	16,885	22,105	12,331	16,399
>Q20 (%)	48.38	51.69	41.64	49.27
>Q30 (%)	15.12	16.77	11.64	15.74
GC (%)	24.9	24.79	27.19	25.08

507 [^]Results presented are from two Nanopore sequencing runs combined

508

509 **Table 3.** Assembly and annotation summary of four isolates from this study, compared to the complete reference sequence for Mycoplasma felis (Myco-2)

Isolate	Myco-2	MF047	MF219	MF329	MF632
Accession	NZAP022325	CP114890	CP114889	CP115656	CP114888
Assembly information					
Length (bp)	841,695	948,716	945,056	936,813	905,741
CheckM completeness (%)	99.21	99.21	99.21	99.21	99.21
PGAP ANI*	98.4%	98.5%	98.6%	98.6%	98.5%
Median sequencing depth					
Short reads	-	1762	1372	467	1499
Long reads	-	695	110	88	181
Genomic features					
CDS	740	759	777	759	743
ncRNA	2	2	2	2	2
rRNA	9	9	9	9	9
Regulatory	2	2	2	2	2
tRNA	29	30	29	29	30
tmRNA	1	1	1	1	1
Genes of interest					
Secretory Systems	0	2	1	3	1
Transposase	22	40	52	27	38

510 * Average nucleotide identity to Mycoplasma felis ATCC 23991 according to internal PGAP ANI taxonomic classification

511

512 **Figure 1.** Coding ratio frequency counts across *Mycoplasma felis* genomes from this study and those currently available
513 on GenBank. Coding ratio determined by dividing amino acid length of annotated proteins to best hit match in custom
514 UniProt Mycoplasma database. Coding ratio axis is log transformed for visualisation. Title names for NCBI origin data
515 includes accession number and strain name (e.g. NZ_CP104194, and 16-040612-4). For Oxford Nanopore only data
516 from NCBI, depth of coverage is added from NCBI (e.g. 58x).

517

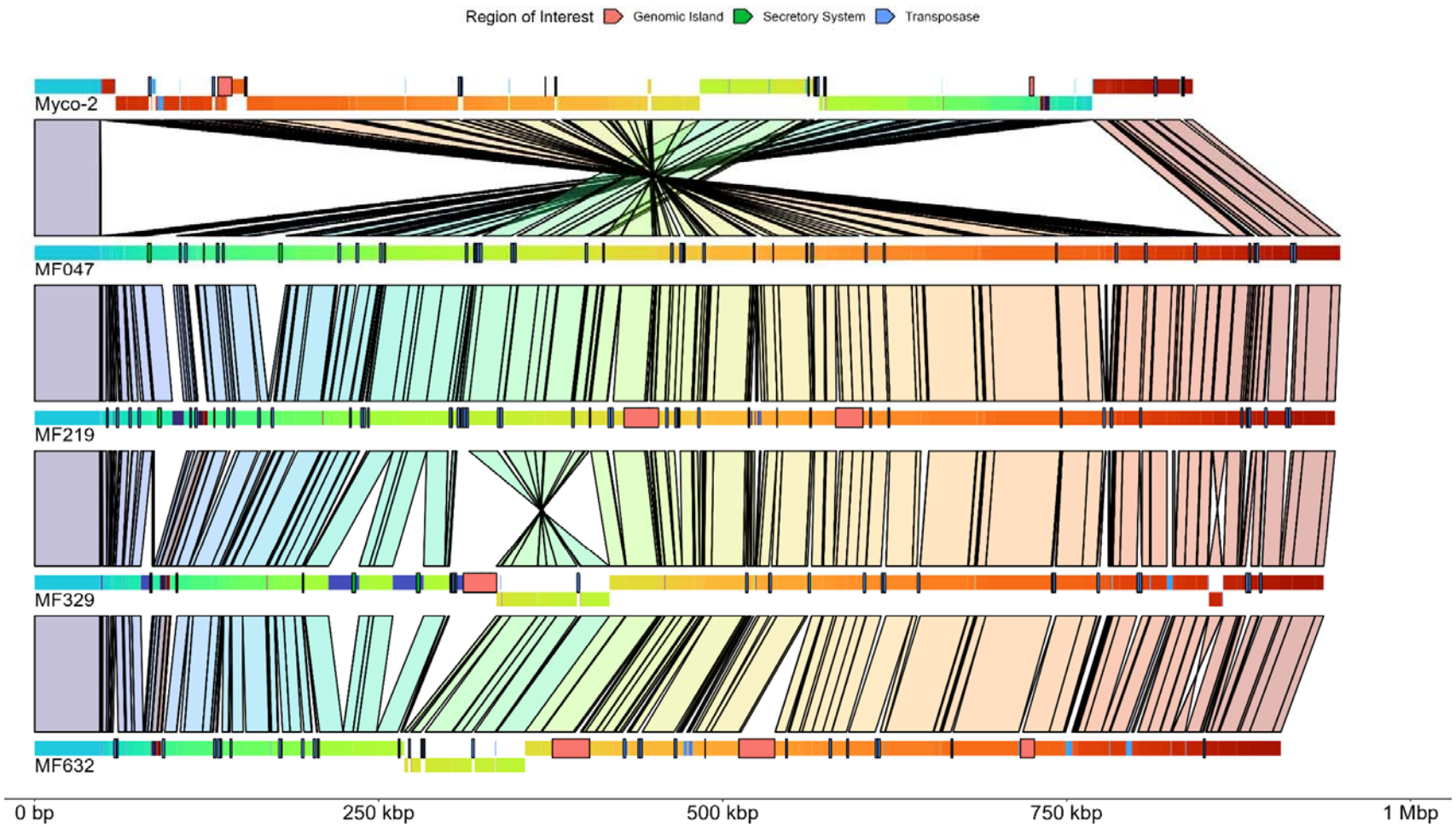

Figure 2. A progressive Mauve alignment of the *Mycoplasma felis* reference genome (Myco-2) and the genomes sequenced in this project. Locally co-linear blocks are separated by colour within genomes, and are the same colour between genomes, with links to identify placement and inversion differences. Solid blocks overlaying the genomes represent the presence of transposases, type IV secretion systems, and genomic islands, whilst solid blocks of blue that break up the colour gradient within the genomes are representative of LCBs not present in linked genomes

524 **Table 4.** Average nucleotide identity (ANI) results of Australian *M. felis* isolate genomes compared to equine reference (Myco-2) and felid contig data sets (Genbank

525 Accessions: MF047: CP114890; MF219: CP114889; MF329: CP115656; MF632: CP114888; Myco-2: AP022325; 16-057065-4: CP103988; 16-040612-4:CP104192;

526 ATCC23391: JNKA01000000).

	MF047	**MF219**	**MF329**	**MF632**	**Myco-2**	**16-057065-4**	**16-040612-4**
MF219	99.79	-	-	-	-	-	-
MF329	98.21	98.16	-	-	-	-	-
MF632	98.21	98.17	98.33	-	-	-	-
Myco-2	98.14	98.06	98.18	98.17	-	-	-
16-057065-4	97.77	97.80	98.25	97.77	97.77	-	-
16-040612-4	97.65	97.65	97.84	97.80	97.72	97.65	-
ATCC23391	98.31	98.29	98.39	98.27	98.33	97.95	97.95

527

528

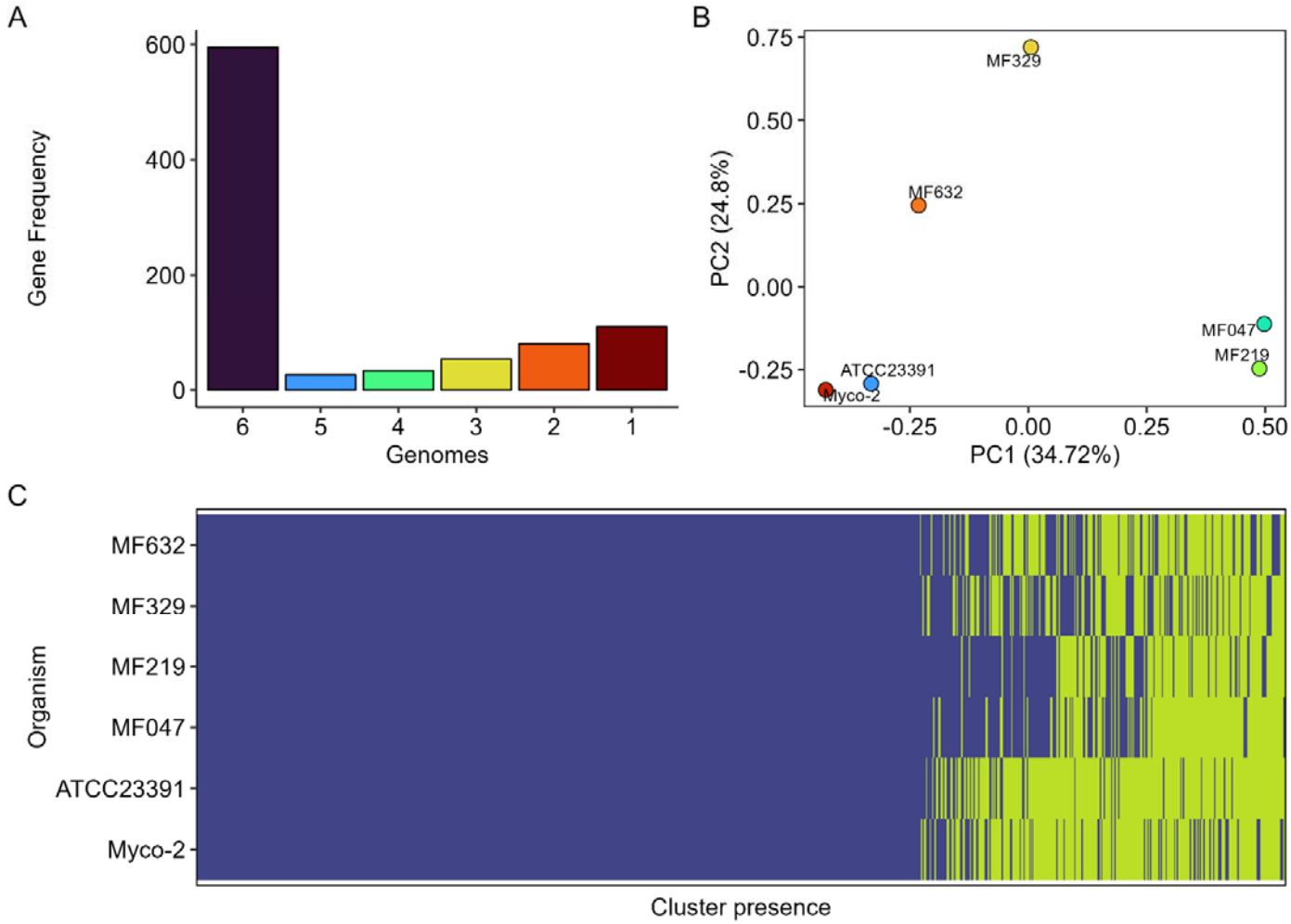

Figure 3. *Mycoplasma felis* core genome and gene presence/absence analysis conducted using Panaroo and plotted using Pagoo. **A)** The frequency of clustered genes within the six genomes used in the analysis. **B)** A principal component analysis of gene presence/absence using Bray Curtis dissimilarity identifies clustering of the previously published genome sequences **C)** Clusters of genes present (blue) or absent (yellow) in the six genomes included in analysis.

533 **Table 5.** Coding sequences detected in the Australian *M. felis* isolate genomes but absent in the equine reference (Myco2), and their possible species of origin based on
534 amino acid sequence identity.

Coding sequence	Possible species of origin	% Amino acid pairwise identity	Predominant Host
Type IV secretory system conjugative DNA transfer family protein	*M. cynos*	43.2	Dog
IS256 family transposase	*M. penetrans*	50.9	Human
Type 2 glycerol-3-phosphate oxidase (GlpO)	*M. canis*	87.2	Dog
PTS fructose transporter subunit IIA	*M. flocculare*	52.6	Swine
DHHA1 domain-containing protein	*M. canis*	84.8	Dog
M13 family peptidase	*M. canis*	65.4	Dog
1-phosphofructokinase family	*M. canis*	52.6	Dog
Anti-termination protein NusB	*M. mustelae*	61.6	Mink
Hsp70 family protein	*M. flocculare*	85.4	Swine
C5 methylase (MAV1virus-like) protein	*M. columboralis*	70.2	Pigeon
16S rRNA methyltransferase (RsmG)	*M. mustelae*	63.3	Mink
HNH endonuclease	*M. columbina*	38.0	Pigeon
Eco47II family restriction endonuclease	*M. mycoides* subsp. *mycoides* SC	49.6	Cattle
Sau3AI family type II restriction endonuclease	*M. crocodyli*	52.7	Crocodile

535

536 **Table 6.** Quantity and range of amino acid identity and similarity of putative virulence and antimicrobial resistance genes (AMR) based on significant BLASTP hits (bit scores
537 >50) compared to the virulence factor database and CARD database, respectively.

Genome	Putative virulence genes			Putative AMR genes		
	Total	Median Identity (min – max)	Median Similarity (min – max)	Total	Median Identity (min – max)	Median Similarity (min – max)
Myco-2	48	31.7 (24.4 - 90.1)	52.6 (44.4 - 95.9)	24	29.8 (22.5 - 40.1)	51.7 (39.1 - 69.6)

Genome	Putative virulence genes			Putative AMR genes		
	Total	Median Identity (min – max)	Median Similarity (min – max)	Total	Median Identity (min – max)	Median Similarity (min – max)
MF047	49	31.6 (24.6 - 90.1)	52.7 (41.8 - 95.9)	25	29.4 (22.6 - 40.3)	50.6 (39.2 - 69.6)
MF219	49	31.6 (24.6 - 90.1)	52.4 (41.8 - 95.9)	25	29.6 (22.6 - 40.3)	50.6 (39.2 - 69.6)
MF329	50	32 (24.4 - 90.1)	52.2 (41.5 - 95.9)	25	29.7 (22.5 - 40.2)	50.6 (39.1 - 69.6)
MF632	51	31.6 (24.4 - 90.1)	52.4 (41.5 - 95.9)	26	29.7 (22.4 - 40.2)	51 (38.9 - 69.6)

538

539

540 **Table 7.** The location of predicted genomic islands in isolated *M. felis* genomes from this study, as well as the reference genome Myco-2. Genomic Islands determined with
541 the Island Finder 4 web tool. None were detected in MF047 isolate.

Strain	Genomic Island	Start – End (Relative to genome)	Length	Total number of genes (non-hypothetical)
Myco-2	1[b,d,e]	133250 - 143277	10027	11 (5)
	2[b,c,d,e]	723039 - 726091	3052	8 (6)
MF047	-	-	-	-
MF219	1[a,b,d,*]	428340 - 453515	25175	15 (7)
	2[a,b,d,e]	582071 - 602042	19971	11 (6)
MF329	1[b,c,#]	311409 - 335810	24401	19 (15)

Strain	Genomic Island	Start – End (Relative to genome)	Length	Total number of genes (non-hypothetical)
MF632	1[a,b,d,*]	376254 - 403316	27062	19 (8)
	2[b,#]	511813 - 537933	26120	22 (15)
	3[a,b,c,d]	716455 - 726594	10139	8 (1)

542 [a, b, c, d, e] – Predicted genomic island is present with some variation, such as the presence/absence of a transposase, in Myco-2 (a), MF047 (b), MF219 (c), MF329 (d), or
543 MF632 (e) but not predicted to be a genomic island in those cases.
544 [*, #] - Predicted genomic islands with structural similarity across different genomes

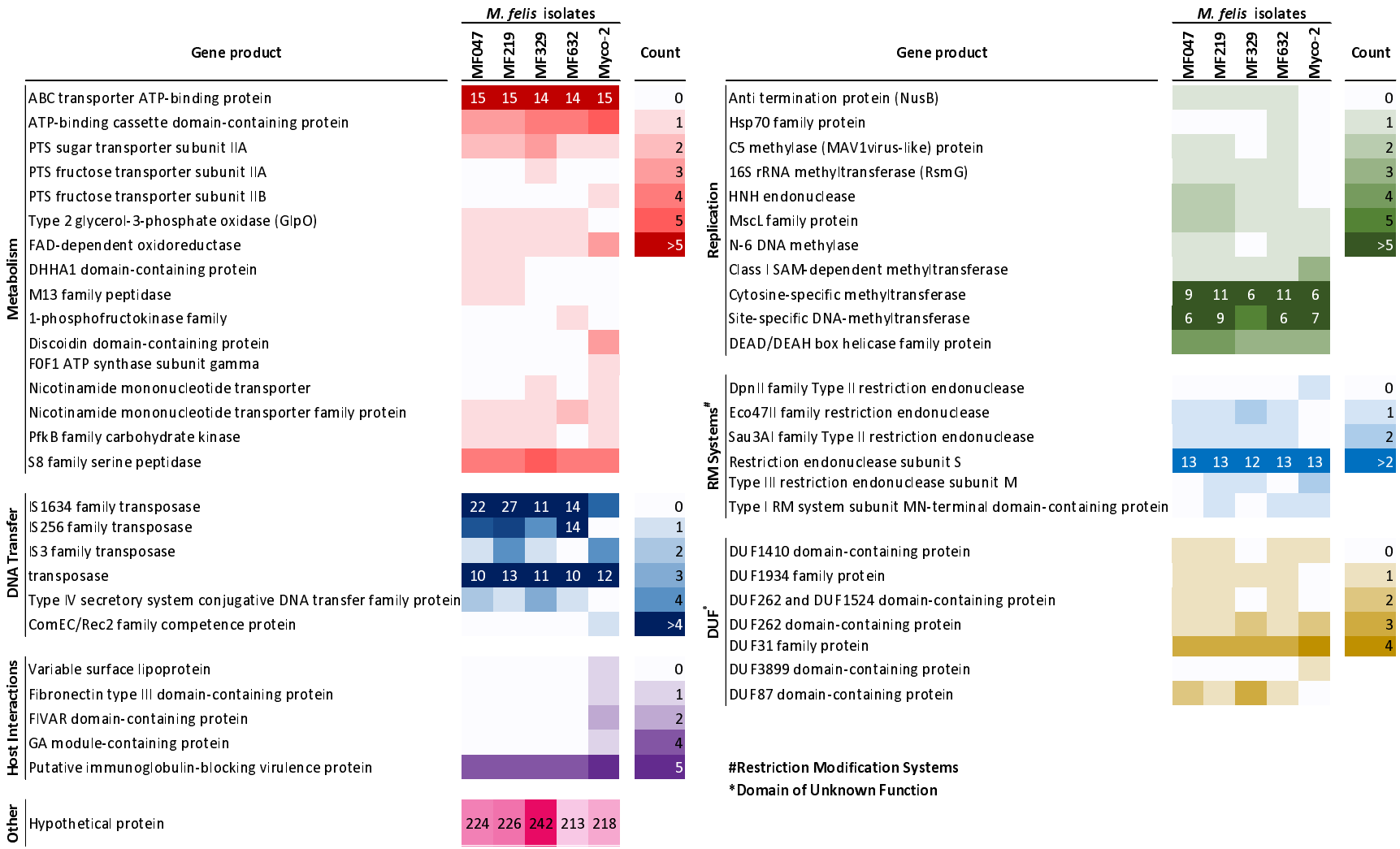

Figure 4. Presence and absence of genes within Australian felid *M. felis* isolates compared to equid *M. felis* reference Myco-2 genome, clustered by putative protein functions. Only genes that differ between isolates or differ from reference are listed. Counts indicate number of gene copies detected within each isolate.

549

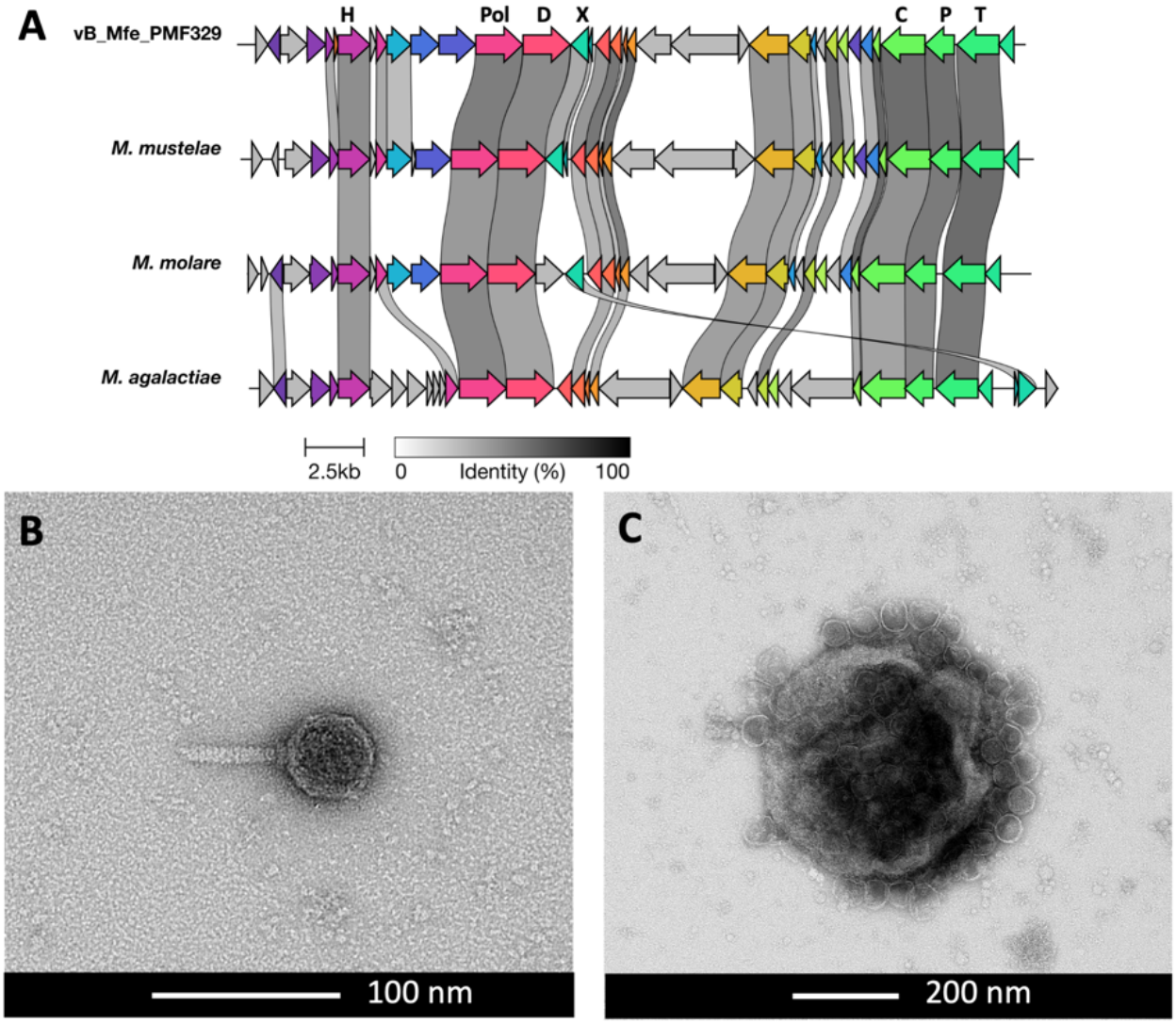

550

551 **Figure 5**. **A)** Genome of bacteriophage identified in *Mycoplasma felis* strain MF329 compared to MAgV1-like prophage
552 sequences found in *M. mustelae*, *M. molare* and *M. agalactiae*. Genome annotations depicting conserved
553 phage/prophage gene sequences are indicated in black. H = Helicase; Pol = DNA polymerase; D = DNA primase; X = Xer
554 recombinase; C = prohead protein; P = portal protein; T = terminase; HP = hypothetical protein. **B)** and **C)** Cryo-
555 transmission electron photomicrographs of bacteriophage detected in cell lysate of *M. felis* isolate MF329 indicating
556 the phage structure consists of a contractile-tail and polyhedral head.

557 ## References:

558 1. **Glass JI, Assad-Garcia N, Alperovich N, Yooseph S, Lewis MR et al.** Essential genes of a
559 minimal bacterium. *Proceedings of the National Academy of Sciences of the United States of*
560 *America* 2006;103(2):425-430.
561 2. **Woese CR, Stackebrandt E, Ludwig W**. What are mycoplasmas: The relationship of tempo
562 and mode in bacterial evolution. *Journal of Molecular Evolution* 1985;21(4):305-316.

563 3. **Fadiel A, Eichenbaum KD, El Semary N, Epperson B**. Mycoplasma genomics: tailoring the
564 genome for minimal life requirements through reductive evolution. *Frontiers in Bioscience-*
565 *Landmark* 2007;12(6):2020-2028.
566 4. **Rocha EPC, Blanchard A**. Genomic repeats, genome plasticity and the dynamics of
567 Mycoplasma evolution. *Nucleic Acids Research* 2002;30(9):2031-2042.
568 5. **Shil PK, Wawegama NK, Browning GF, Noormohammadi AH, Marenda MS**. Mycoplasmas.
569 In: J.F. Prescott, A.N. Rycroft, J.D. Boyce, J.I. MacInnes, Immerseel FV et al. (editors). *Pathogenesis*
570 *of Bacterial Infections in Animals* 2022. pp. 667-700.
571 6. **Krause DC, Leith DK, Wilson RM, Baseman JB**. Identification of *Mycoplasma pneumoniae*
572 proteins associated with hemadsorption and virulence. *Infect Immun* 1982;35(3):809-817.
573 7. **Delaney NF, Balenger S, Bonneaud C, Marx CJ, Hill GE et al.** Ultrafast evolution and loss of
574 CRISPRs following a host shift in a novel wildlife pathogen, *Mycoplasma gallisepticum*. *PLOS*
575 *Genetics* 2012;8(2):e1002511.
576 8. **Momynaliev KT, Govorun VM**. Mechanisms of genetic instability in Mollicutes
577 (Mycoplasmas). *Russian Journal of Genetics* 2001;37(9):979-992.
578 9. **Citti C, Dordet-Frisoni E, Nouvel LX, Kuo CH, Baranowski E**. Horizontal Gene Transfers in
579 Mycoplasmas (Mollicutes). *Current Issues in Molecular Biology* 2018;29(1):3-22.
580 10. **Klose SM, Olaogun OM, Disint JF, Shil P, Gyuranecz M et al.** Genomic diversity of a globally
581 used, live attenuated mycoplasma vaccine. *Microbiology Spectrum* 2022;10(6):e02845-02822.
582 11. **Klose SM, Shil P, Underwood GJ, Morrow CJ, Marenda MS et al.** Obg plays a significant role
583 in temperature sensitivity of Mycoplasma synoviae live attenuated vaccine strain MS-H. *Veterinary*
584 *Microbiology* 2023:109818.
585 12. **Klose SM, Omotainse OS, Zare S, Vaz PK, Armat P et al.** Virulence factors of Mycoplasma
586 synoviae: Three genes influencing colonization, immunogenicity, and transmissibility. *Frontiers in*
587 *Microbiology* 2022;13:1042212.
588 13. **Klose SM, De Souza DP, Disint JF, Andrews DM, Underwood GJ et al.** Reversion of
589 mutations in a live mycoplasma vaccine alters its metabolism. *Vaccine* 2023;41(21):3358-3366.
590 14. **Noormohammadi A, Markham P, Duffy M, Whithear K, Browning G**. Multigene families
591 encoding the major hemagglutinins in phylogenetically distinct mycoplasmas. *Infection and*
592 *Immunity* 1998;66(7):3470-3475.
593 15. **Sirand-Pugnet P, Lartigue C, Marenda M, Jacob D, Barré A et al.** Being pathogenic, plastic,
594 and sexual while living with a nearly minimal bacterial genome. *PLOS Genetics* 2007;3(5):e75.
595 16. **Randolph J, Moise N, Scarlett J, Shin S, Blue J et al.** Prevalence of mycoplasmal and
596 ureaplasmal recovery from tracheobronchial lavages and of mycoplasmal recovery from pharyngeal
597 swab specimens in cats with or without pulmonary disease. *American journal of veterinary research*
598 1993;54(6):897-900.
599 17. **Foster S, Barrs V, Martin P, Malik R**. Pneumonia associated with *Mycoplasma* spp in three
600 cats. *Australian veterinary journal* 1998;76(7):460-464.
601 18. **Sykes JE**. Feline hemotropic mycoplasmas. *Journal of Veterinary Emergency and Critical Care*
602 2010;20(1):62-69.
603 19. **Le Boedec K**. A systematic review and meta-analysis of the association between
604 Mycoplasma spp and upper and lower respiratory tract disease in cats. *Journal of the American*
605 *Veterinary Medical Association* 2017;250(4):397-407.
606 20. **Cohn LA**. Feline respiratory disease complex. *Veterinary Clinics: Small Animal Practice*
607 2011;41(6):1273-1289.
608 21. **Nguyen D, Barrs VR, Kelman M, Ward MP**. Feline upper respiratory tract infection and
609 disease in Australia. *Journal of Feline Medicine and Surgery* 2019;21(10):973-978.

610 22. **Fernandez M, Manzanilla EG, Lloret A, León M, Thibault J-C**. Prevalence of feline
611 herpesvirus-1, feline calicivirus, *Chlamydophila felis* and *Mycoplasma felis* DNA and associated risk
612 factors in cats in Spain with upper respiratory tract disease, conjunctivitis and/or gingivostomatitis.
613 *Journal of Feline Medicine and Surgery* 2017;19(4):461-469.
614 23. **Lee-Fowler T**. Feline respiratory disease: What is the role of Mycoplasma species? *Journal of*
615 *Feline Medicine and Surgery* 2014;16(7):563-571.
616 24. **Tonozzi CC**. *Feline Respiratory Disease Complex*. MSD Veterinary Manual 2022.
617 25. **Kinoshita Y, Niwa H, Uchida-Fujii E, Nukada T**. Complete genome sequence of mycoplasma
618 felis Strain Myco-2, isolated from an equine tracheal wash sample in Japan. *Microbiology Resource*
619 *Announcements* 2020;9(9):10.1128/mra. 00057-00020.
620 26. **Framst I, D`Andrea C, Baquero M, Maboni G**. Development of a long-read next generation
621 sequencing workflow for improved characterization of fastidious respiratory mycoplasmas.
622 *Microbiology* 2022;168(11).
623 27. **Frey M**. A medium for the isolation of avian mycoplasmas. *American Journal of Veterinary*
624 *Research* 1968;29:2163-2171.
625 28. **Klose SM, Omotainse OS, Zare S, Vaz PK, Armat P et al.** Virulence factors of Mycoplasma
626 synoviae: Three genes influencing colonization, immunogenicity, and transmissibility. *Front*
627 *Microbiol*, Original Research 2022;13.
628 29. **Chen S, Zhou Y, Chen Y, Gu J**. fastp: an ultra-fast all-in-one FASTQ preprocessor.
629 *Bioinformatics* 2018;34(17):i884-i890.
630 30. **Wick R**. *Filtlong v. 0.2. 0*. 2021.
631 31. **Wick RR, Judd LM, Gorrie CL, Holt KE**. Unicycler: Resolving bacterial genome assemblies
632 from short and long sequencing reads. *PLOS Computational Biology* 2017;13(6):e1005595.
633 32. **Wick RR, Holt KE**. Polypolish: Short-read polishing of long-read bacterial genome
634 assemblies. *PLOS Computational Biology* 2022;18(1):e1009802.
635 33. **Li H**. Aligning sequence reads, clone sequences and assembly contigs with BWA-MEM. *arXiv*
636 *preprint arXiv:13033997* 2013.
637 34. **Darling AE, Mau B, Perna NT**. Progressive Mauve: Multiple alignment of genomes with gene
638 flux and rearrangement. *arXiv preprint arXiv:09105780* 2009.
639 35. **Tatusova T, DiCuccio M, Badretdin A, Chetvernin V, Nawrocki EP et al.** NCBI prokaryotic
640 genome annotation pipeline. *Nucleic Acids Research* 2016;44(14):6614-6624.
641 36. **Buchfink B, Reuter K, Drost H-G**. Sensitive protein alignments at tree-of-life scale using
642 DIAMOND. *Nature Methods* 2021;18(4):366-368.
643 37. **Tonkin-Hill G, MacAlasdair N, Ruis C, Weimann A, Horesh G et al.** Producing polished
644 prokaryotic pangenomes with the Panaroo pipeline. *Genome Biology* 2020;21(1):180.
645 38. **Ferrés I, Iraola G**. An object-oriented framework for evolutionary pangenome analysis. *Cell*
646 *Reports Methods* 2021;1(5):100085.
647 39. **Dhillon BK, Chiu TA, Laird MR, Langille MG, Brinkman FS**. IslandViewer update: improved
648 genomic island discovery and visualization. *Nucleic Acids Research* 2013;41(W1):W129-W132.
649 40. **Liu M, Li X, Xie Y, Bi D, Sun J et al.** ICEberg 2.0: an updated database of bacterial integrative
650 and conjugative elements. *Nucleic Acids Research* 2018;47(D1):D660-D665.
651 41. **Alcock BP, Huynh W, Chalil R, Smith KW, Raphenya AR et al.** CARD 2023: expanded
652 curation, support for machine learning, and resistome prediction at the Comprehensive Antibiotic
653 Resistance Database. *Nucleic Acids Research* 2023;51(D1):D690-D699.
654 42. **Liu B, Zheng D, Zhou S, Chen L, Yang J**. VFDB 2022: a general classification scheme for
655 bacterial virulence factors. *Nucleic acids research* 2022;50(D1):D912-D917.

656 43. **Li H**. Minimap2: pairwise alignment for nucleotide sequences. *Bioinformatics*
657 2018;34(18):3094-3100.
658 44. **Garneau JR, Depardieu F, Fortier L-C, Bikard D, Monot M**. PhageTerm: a tool for fast and
659 accurate determination of phage termini and packaging mechanism using next-generation
660 sequencing data. *Scientific Reports* 2017;7(1):8292.
661 45. **Parks DH, Imelfort M, Skennerton CT, Hugenholtz P, Tyson GW**. CheckM: assessing the
662 quality of microbial genomes recovered from isolates, single cells, and metagenomes. *Genome*
663 *Research* 2015;25(7):1043-1055.
664 46. **Nishimura Y, Yoshida T, Kuronishi M, Uehara H, Ogata H et al.** ViPTree: the viral proteomic
665 tree server. *Bioinformatics* 2017;33(15):2379-2380.
666 47. **Bin Jang H, Bolduc B, Zablocki O, Kuhn JH, Roux S et al.** Taxonomic assignment of
667 uncultivated prokaryotic virus genomes is enabled by gene-sharing networks. *Nature Biotechnology*
668 2019;37(6):632-639.
669 48. **Citti C, Baranowski E, Dordet-Frisoni E, Faucher M, Nouvel L-X**. Genomic Islands in
670 Mycoplasmas. *Genes* 2020;11(8):836.
671 49. **Gourlay RN, Wyld SG, Garwes DJ**. Some properties of mycoplasma virus Br1. *Archives of*
672 *Virology* 1983;75(1):1-15.
673 50. **Gourlay RN, Wyld SG, Poulton ME**. Some characteristics of Mycoplasma virus Hr1, isolated
674 from and infectingMycoplasma hyorhinis. *Archives of Virology* 1983;77(1):81-85.
675 51. **Mahillon J, Chandler M**. Insertion sequences. *Microbiology and Molecular Biology Reviews*
676 1998;62(3):725-774.
677 52. **Frey J**. Insertion Sequence Analysis. In: Miles R, Nicholas R (editors). *Mycoplasma Protocols*.
678 Totowa, NJ: Humana Press; 1998. pp. 197-205.
679 53. **Lysnyansky I, Calcutt MJ, Ben-Barak I, Ron Y, Levisohn S et al.** Molecular characterization of
680 newly identified IS 3, IS 4 and IS 30 insertion sequence-like elements in Mycoplasma bovis and their
681 possible roles in genome plasticity. *FEMS microbiology letters* 2009;294(2):172-182.
682 54. **Thomas A, Linden A, Mainil J, Bischof DF, Frey J et al.** Mycoplasma bovis shares insertion
683 sequences with Mycoplasma agalactiae and Mycoplasma mycoides subsp. mycoides SC:
684 Evolutionary and developmental aspects. *FEMS Microbiology Letters* 2005;245(2):249-255.
685 55. **Loreto ELS, Ortiz MF, Porto JIR**. Insertion sequences as variability generators in the
686 Mycoplasma hyopneumoniae and M. synoviae genomes. *Genetics and Molecular Biology*
687 2007;30:283-289.
688 56. **Vilei EM, Nicolet J, Frey J**. IS*1634*, a novel insertion element creating long, variable-length
689 direct repeats which is specific for *Mycoplasma mycoides* subsp. *mycoides* small-colony type.
690 *Journal of Bacteriology* 1999;181(4):1319-1323.
691 57. **Baranowski E, Dordet-Frisoni E, Sagné E, Hygonenq M-C, Pretre G et al.** The Integrative
692 Conjugative Element (ICE) of *Mycoplasma agalactiae*: Key Elements Involved in Horizontal
693 Dissemination and Influence of Coresident ICEs. *mBio* 2018;9(4):10.1128/mbio.00873-00818.
694 58. **Alvarez-Martinez CE, Christie PJ**. Biological Diversity of Prokaryotic Type IV Secretion
695 Systems. *Microbiology and Molecular Biology Reviews* 2009;73(4):775-808.
696 59. **Dordet-Frisoni E, Sagné E, Baranowski E, Breton M, Nouvel LX et al.** Chromosomal transfers
697 in mycoplasmas: when minimal genomes go mobile. *MBio* 2014;5(6):10.1128/mbio. 01958-01914.
698 60. **Hartmann AD, Hawley J, Werckenthin C, Lappin MR, Hartmann K**. Detection of bacterial
699 and viral organisms from the conjunctiva of cats with conjunctivitis and upper respiratory tract
700 disease. *Journal of Feline Medicine & Surgery* 2010;12(10):775-782.
701 61. **Ahmer BMM, Tran M, Heffron F**. The virulence plasmid of *Salmonella typhimurium* is self-
702 transmissible. *Journal of Bacteriology* 1999;181(4):1364-1368.

703 62. **Szczepanek SM, Boccaccio M, Pflaum K, Liao X, Geary SJ**. Hydrogen Peroxide Production
704 from Glycerol Metabolism Is Dispensable for Virulence of Mycoplasma gallisepticum in the Tracheas
705 of Chickens. *Infection and Immunity* 2014;82(12):4915-4920.
706 63. **Hames C, Halbedel S, Hoppert M, Frey J, Stülke J**. Glycerol metabolism is important for
707 cytotoxicity of Mycoplasma pneumoniae. *Journal of Bacteriology* 2009;191(3):747-753.
708 64. **Chang T-H, Lo W-S, Ku C, Chen L-L, Kuo C-H**. Molecular evolution of the substrate utilization
709 strategies and putative virulence factors in mosquito-associated Spiroplasma species. *Genome*
710 *Biology and Evolution* 2014;6(3):500-509.
711 65. **Pilo P, Vilei EM, Peterhans E, Bonvin-Klotz L, Stoffel MH et al.** A metabolic enzyme as a
712 primary virulence factor of Mycoplasma mycoides subsp. mycoides small colony. *Journal of*
713 *bacteriology* 2005;187(19):6824-6831.
714 66. **Khan LA, Miles RJ, Nicholas RAJ**. Hydrogen Peroxide Production by Mycoplasma bovis and
715 Mycoplasma agalactiae and Effect of In Vitro Passage on a Mycoplasma bovis Strain Producing High
716 Levels of H2O2. *Veterinary Research Communications* 2005;29(3):181-188.
717 67. **Szczepanek S, Tulman E, Gorton T, Liao X, Lu Z et al.** Comparative genomic analyses of
718 attenuated strains of Mycoplasma gallisepticum. *Infection and immunity* 2010;78(4):1760-1771.
719 68. **Tseng C-W, Chiu C-J, Kanci A, Citti C, Rosengarten R et al.** The oppD gene and putative
720 peptidase genes may be required for virulence in Mycoplasma gallisepticum. *Infection and*
721 *Immunity* 2017;85(6):10.1128/iai. 00023-00017.
722 69. **Masukagami Y, Nijagal B, Mahdizadeh S, Tseng C-W, Dayalan S et al.** A combined
723 metabolomic and bioinformatic approach to investigate the function of transport proteins of the
724 important pathogen Mycoplasma bovis. *Veterinary microbiology* 2019;234:8-16.
725 70. **Masukagami Y, De Souza D, Dayalan S, Bowen C, O'callaghan S et al.** Comparative
726 metabolomics of Mycoplasma bovis and Mycoplasma gallisepticum reveals fundamental
727 differences in active metabolic pathways and suggests novel gene annotations. *MSystems*
728 2017;2(5):10.1128/msystems. 00055-00017.
729 71. **Mahdizadeh S, Masukagami Y, Tseng C-W, Markham PF, De Souza DP et al.** A *Mycoplasma*
730 *gallisepticum* glycerol ABC transporter involved in pathogenicity. *Applied and Environmental*
731 *Microbiology* 2021;87(11):e03112-03120.
732 72. **Chen H, Yu S, Shen X, Chen D, Qiu X et al.** The Mycoplasma gallisepticum α-enolase is cell
733 surface-exposed and mediates adherence by binding to chicken plasminogen. *Microbial*
734 *Pathogenesis* 2011;51(4):285-290.
735 73. **Vilei EM, Frey J**. Genetic and biochemical characterization of glycerol uptake in Mycoplasma
736 mycoides subsp. mycoides sc: Its impact on h2o2production and virulence. *Clinical Diagnostic*
737 *Laboratory Immunology* 2001;8(1):85-92.
738 74. **Shterzer N, Mizrahi I**. The animal gut as a melting pot for horizontal gene transfer. *Canadian*
739 *Journal of Microbiology* 2015;61(9):603-605.
740 75. **Norman A, Hansen LH, Sørensen SJ**. Conjugative plasmids: vessels of the communal gene
741 pool. *Philosophical Transactions of the Royal Society B: Biological Sciences* 2009;364(1527):2275-
742 2289.
743 76. **Oliveira PH, Touchon M, Rocha EP**. The interplay of restriction-modification systems with
744 mobile genetic elements and their prokaryotic hosts. *Nucleic acids research* 2014;42(16):10618-
745 10631.
746 77. **Dordet-Frisoni E, Vandecasteele C, Contarin R, Sagné E, Baranowski E et al.** Impacts of
747 *Mycoplasma agalactiae* restriction-modification systems on pan-epigenome dynamics and genome
748 plasticity. *Microbial Genomics* 2022;8(5).

749 78. **Oliveira PH, Touchon M, Rocha EPC**. Regulation of genetic flux between bacteria by
750 restriction–modification systems. *Proceedings of the National Academy of Sciences*
751 2016;113(20):5658-5663.
752 79. **Chen I, Dubnau D**. DNA uptake during bacterial transformation. *Nature Reviews*
753 *Microbiology* 2004;2(3):241-249.
754 80. **Kapteijn R, Shitut S, Aschmann D, Zhang L, de Beer M et al.** Endocytosis-like DNA uptake by
755 cell wall-deficient bacteria. *Nature Communications* 2022;13(1):5524.
756 81. **Pimentel ZT, Zhang Y**. Evolution of the natural transformation protein, ComEC, in bacteria.
757 *Frontiers in Microbiology* 2018:2980.
758 82. **Wang Y, Huang JM, Wang SL, Gao ZM, Zhang AQ et al.** Genomic characterization of
759 symbiotic mycoplasmas from the stomach of deep-sea isopod Bathynomus sp. *Environmental*
760 *Microbiology* 2016;18(8):2646-2659.
761 83. **Christner M, Franke GC, Schommer NN, Wendt U, Wegert K et al.** The giant extracellular
762 matrix-binding protein of *Staphylococcus epidermidis* mediates biofilm accumulation and
763 attachment to fibronectin. *Molecular Microbiology* 2010;75(1):187-207.
764 84. **Speziale P, Pietrocola G, Foster TJ, Geoghegan JA**. Protein-based biofilm matrices in
765 Staphylococci. *Frontiers in cellular and infection microbiology* 2014;4:171.
766 85. **Ledger L, Eidt J, Cai HY**. Identification of antimicrobial resistance-associated genes through
767 whole genome sequencing of *Mycoplasma bovis* isolates with different antimicrobial resistances.
768 *Pathogens* 2020;9(7):588.
769 86. **Mahdizadeh S, Sansom FM, Lee S-W, Browning GF, Marenda MS**. Targeted mutagenesis of
770 *Mycoplasma gallisepticum* using its endogenous CRISPR/Cas system. *Veterinary Microbiology*
771 2020;250:108868.
772 87. **Pereyre S, Goret J, Bébéar C**. *Mycoplasma pneumoniae*: current knowledge on macrolide
773 resistance and treatment. *Frontiers in Microbiology* 2016;7:974.
774 88. **Dégrange S, Renaudin H, Charron A, Pereyre S, Bébéar C et al.** Reduced susceptibility to
775 tetracyclines is associated *in vitro* with the presence of 16S rRNA mutations in *Mycoplasma hominis*
776 and *Mycoplasma pneumoniae*. *Journal of antimicrobial chemotherapy* 2008;61(6):1390-1392.
777 89. **Shimada Y, Deguchi T, Nakane K, Yasuda M, Yokoi S et al.** Macrolide resistance–associated
778 23S rRNA mutation in *Mycoplasma genitalium*, Japan. *Emerging infectious diseases*
779 2011;17(6):1148.
780 90. **Kovács ÁB, Wehmann E, Sváb D, Bekő K, Grózner D et al.** Novel prophage-like sequences in
781 *Mycoplasma anserisalpingitidis*. *Infection, Genetics and Evolution* 2021;92:104886.
782 91. **Turner D, Shkoporov AN, Lood C, Millard AD, Dutilh BE et al.** Abolishment of morphology-
783 based taxa and change to binomial species names: 2022 taxonomy update of the ICTV bacterial
784 viruses subcommittee. *Archives of Virology* 2023;168(2):74.
785 92. **Röske K, Calcutt MJ, Wise KS**. The Mycoplasma fermentans prophage ϕMFV1: genome
786 organization, mobility and variable expression of an encoded surface protein. *Molecular*
787 *Microbiology* 2004;52(6):1703-1720.
788